

Supporting Information

(i) SPIONs

Absorbance properties of SPIONs are shown in Figure S1 (a). 200 mesh copper TEM grids were prepared by covering with a layer of formvar followed by a carbon coating. A 4 μL volume of a 25 $\mu\text{g}/\text{mL}$ SPION solution (in water) was deposited directly onto the grid and left to dry overnight before imaging using an FEI Technai G² Spirit BioTwin electron microscope operated at 100 kV and can be seen in Figure S1 (c).

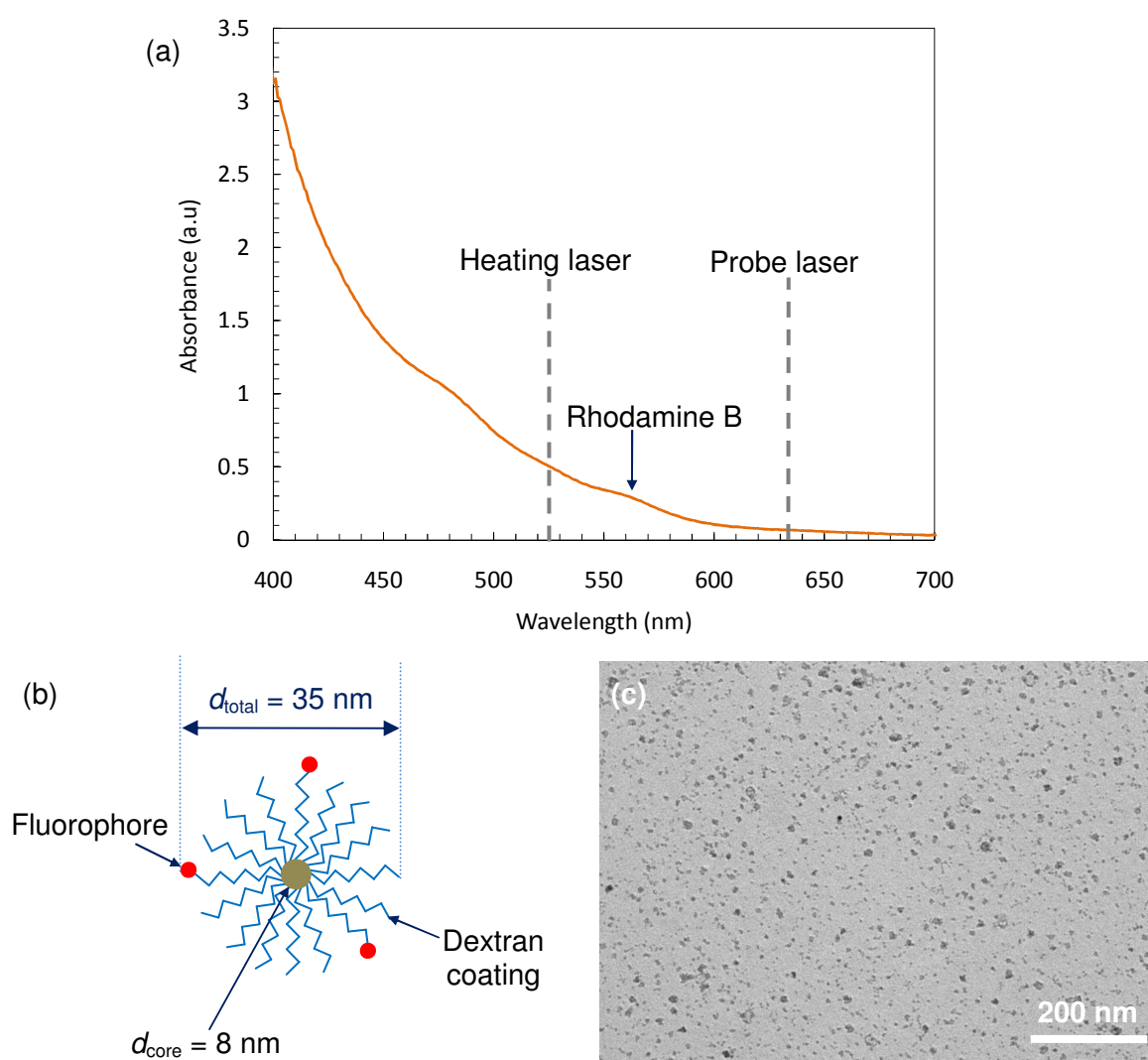


Figure S1. Absorbance spectrum of Molday ION in water. The wavelengths of the heating and probe lasers used in photothermal imaging are indicated. (b) Schematic representation of Molday ION particles and (c) transmission electron micrograph of SPIONs deposited directly onto TEM grids.

(ii) Fluorescence and photothermal imaging

Fluorescence and photothermal imaging was performed using the set-up shown in Figure S2.

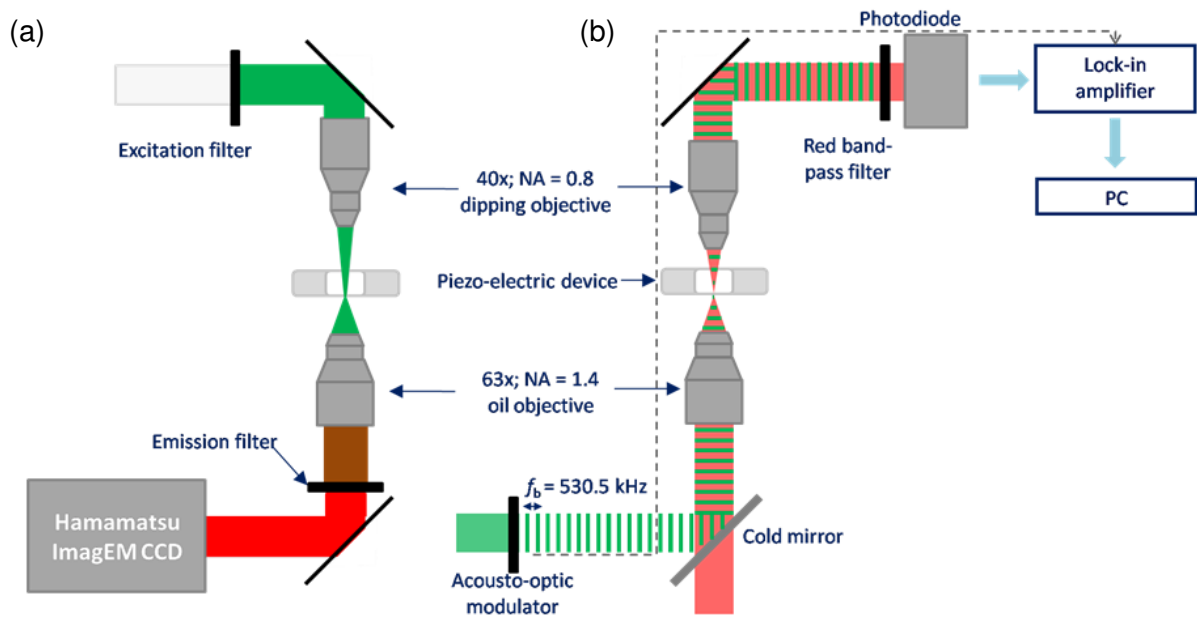


Figure S2. Simplified schematic representations of the set up used to measure (a) fluorescence and (b) photothermal imaging of SPIONs in cells. In (b), the heating laser (*green*) is modulated by an acousto-optical modulator at a frequency of 530.5 kHz; the green laser is blocked before the photodiode, which measures the signal of the probe (*red*) beam only. A lock-in amplifier is used to extract the magnitude of the signal at the beatnote frequency, which is digitised to yield the photothermal signal. The system is based upon a modified Zeiss Axiovert 200 inverted microscope equipped with a microscope cage incubator.

(iii) Sensitivity of photothermal signal to SPIONs

Figure S3 presents larger image of the drop imaged using fluorescence images taken before and after scanning with the photothermal. The scanned areas are indicated by squares. Photobleaching of the scanned areas is clearly visible, further confirming that we are indeed imaging SPIONs.

We have estimated the number of SPIONs our set up is sensitive using the following calculations. According to the manufacturer, each SPION core has a nominal diameter of 8 nm. Assuming all particles are spherical, the volume of an individual SPION of radius r is given by:

$$\frac{4}{3} \pi r^3 = 2.68 \times 10^{-19} \text{ cm}^3 \quad \text{Equation 1}$$

The mass of iron per SPION can be calculated if the density of iron oxide is known. There are no details given by the manufacturer regarding the precise iron oxide species, and so we have assumed it is all Fe_3O_4 , which exists as $\text{FeO} \cdot \text{Fe}_2\text{O}_3$. As there are no details of the stoichiometry of these phases, we will use physical properties of Fe_3O_4 for the remainder of the calculations.

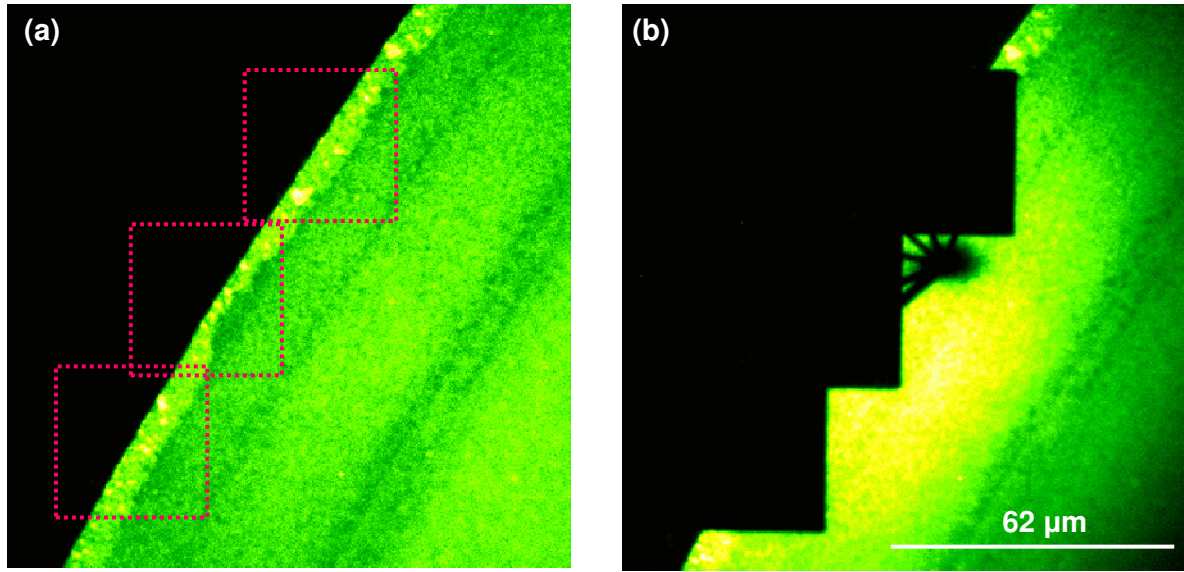


Figure S3. Fluorescence images of edge of drop (a) pre-photothermal imaging and (b) post-photothermal imaging. The scanned regions are indicated by the squares in (a), and have been photobleached by in (b). The black spot in (b) corresponds to the position of the laser before scanning, with the lines associated with the Piezo scanner moving to the starting position of the laser.

Using a density of Fe_3O_4 , $\rho_{\text{Fe}_3\text{O}_4}$ as 5.24 g/cm^3 (taken fromⁱ), combined with molecular mass of 231.54 g/mol , the mass of iron per SPION can be deduced using:

$$m_{\text{Fe}} = \left(\frac{3M_{\text{Fe}}}{M_{\text{Fe}_3\text{O}_4}} \right) \cdot \rho_{\text{Fe}_3\text{O}_4} V_{\text{SPION}} = 1.01 \times 10^{-18} \text{ g} \quad \text{Equation 2}$$

Where M is the molecular mass, ρ is the density and V is the volume, respectively.

The measurements presented in Figure 1 were obtained using a $5 \mu\text{L}$ drop of $20 \mu\text{g/mL}$ SPIONs corresponds to 100 ng SPIONs. As the concentration of SPIONs given by the manufacturer corresponds to the concentration of iron only, the number of SPIONs in a 100 ng solution can be calculated *via*:

$$\frac{\text{Total mass of iron}}{\text{Mass of iron per SPION}} = \frac{100 \times 10^{-9} \text{ g}}{1.01 \times 10^{-18} \text{ g}} = 9.9 \times 10^{10} \text{ SPIONs} \quad \text{Equation 3}$$

In order to establish the surface density of SPIONs, we now need to calculate the surface area of the drop adsorbed to the surface. The drop was measured to be 3 mm ; assuming this to be perfecting circular, then this corresponds to a surface area of $7.07 \times 10^{-6} \text{ m}^2$. Further assuming that all the SPIONs present in the drop adsorbed to the surface, the surface density of SPIONs is given by:

$$\text{Surface density of SPIONs} = \frac{9.9 \times 10^{10} \text{ SPIONs}}{7.07 \times 10^{-6} \text{ m}^2} = 1.4 \times 10^{16} \text{ SPIONs/m}^2 \quad \text{Equation 4}$$

It makes more sense to express this in $\text{SPIONs}/\mu\text{m}^2$, which is given as:

$$\text{Surface density of SPIONs} = 1.4 \times 10^{16} \text{SPIONs/m}^2 = 1.4 \times 10^4 \text{SPIONs/}\mu\text{m}^2 \quad \text{Equation 5}$$

The detection threshold of our system can be estimated using the line profile in Figure 1 (c) and using the following calculations. The mean background signal is (89.62 ± 9.32) counts, whilst in the area of the homogeneous SPIONs the mean signal increases to 209.05 counts. We define the limit of detection as:

$$\text{Limit of detection} = 3\sigma = (3 \times 9.32) = 27.96 \quad \text{Equation 6}$$

Where σ is the standard deviation of the background. If we assume that there is a linear relation between the signal (in counts) and the number of SPIONs then:

$$\begin{aligned} 209.05 &\equiv 1.4 \times 10^{16} \text{SPIONs/m}^2 \\ 27.96 &\equiv 1.9 \times 10^{15} \text{SPIONs/m}^2 \end{aligned} \quad \text{Equation 7}$$

Finally, the number of SPIONs detected can be deduced by calculating the surface area 'seen' by the lasers, which is approximately given by $\frac{\lambda}{2}$;

$$\text{Limit of detection} = (1.9 \times 10^{15} \text{SPIONs/m}^2) \cdot (2.8 \times 10^{-13} \text{m}^2) \approx 530 \text{ SPIONs} \quad \text{Equation 8}$$

(iv) TEM micrographs of fixed cells containing SPIONs

TEM micrographs presented in Figure S4 shows that there are large numbers of SPIONs in each vesicle. To prepare sections, the labelled cells were fixed with 4% PFA and 2.5% glutaraldehyde in 0.1 M phosphate buffer, osmicated and processed for epoxy resin embedding. Then, 70 nm sections were obtained with an ultramicrotome and collected over copper grids containing a formvar support film.

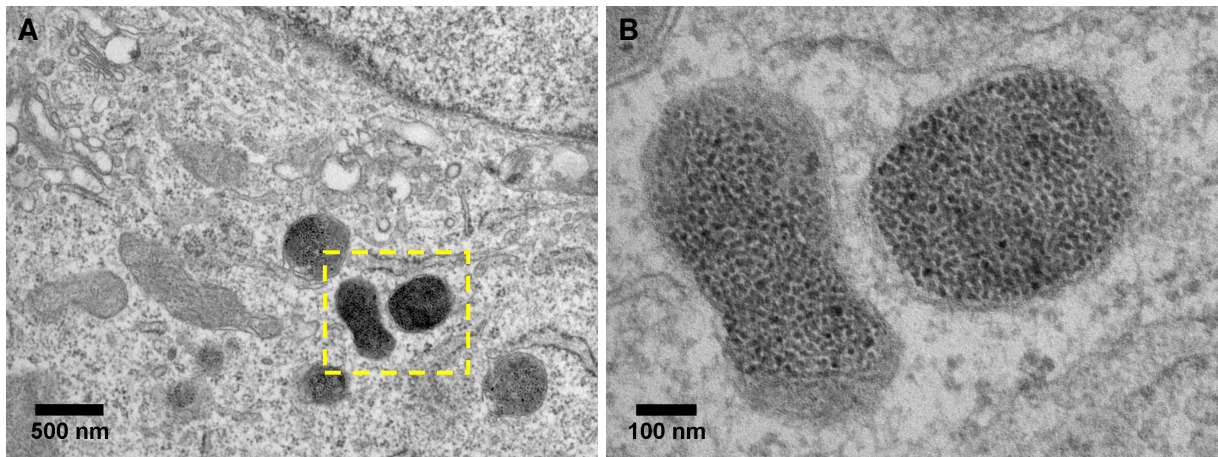


Figure S4. Transmission electron micrographs of cells incubated with 5 $\mu\text{g/mL}$ Molday ION for 24 h at a magnification of 8200x (*left*) and 26000x (*right*). The image presented in B corresponds to the area highlighted in the square in A. The nucleus can be clearly seen in the top right hand of image A.

The sections were finally stained with 5% uranyl acetate and 2% lead citrate. Electron microscopy was performed using an FEI Technai G² Spirit BioTwin electron microscope operated at 100 kV.

(v) Single cell analysis for quantification of photothermal signal

Quantification of the photothermal signal was performed using a single cell analysis using MacBiophotonics Image J. For each field, each full cell was outlined using the freehand polygon selection, as shown in Figure S5, and added to the region of interest manager. In addition, the mean background intensity for each field was measured by measuring the signal in at least three areas without cells. The mean signal per field was obtained by taking the mean signal of each cell, and subtracting the mean value of the background signal. Finally, the mean signal per condition was obtained by taking the mean of the each field values. At least 50 cells on at least 7 different fields were analysed per condition.

We have estimated the mean amount of iron per cell required for quantification *via* the photothermal technique using a similar approach given in section (iii), as shown by the following calculations. The background photothermal signal detected from cells only is given in Table 1 as 4.92 mV, with a standard deviation, σ , of 1.93. As before, we define the limit of detection as 3σ , then the threshold for photothermal detection is given by:

$$\text{Limit of detection} = 3\sigma = 3 \times 1.93 = 5.79 \text{ mV} \quad \text{Equation 9}$$

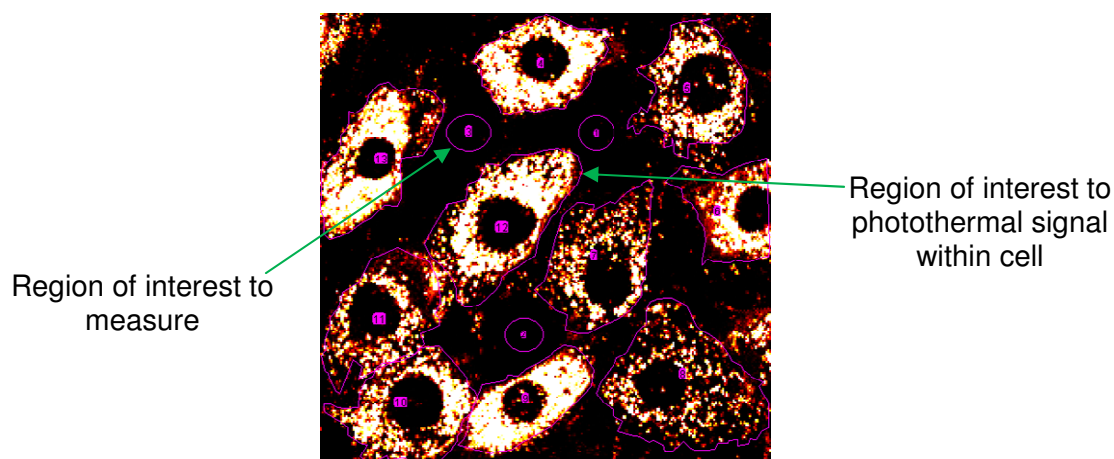


Figure S5. Cell outlines used for single cell analysis to quantify the photothermal signal per cell for cells incubated with 5 $\mu\text{g/mL}$ SPIONs.

We can deduce the amount of iron this corresponds to by using the line of best fit in Figure 3 (b):

$$\text{PhT (mV)} = (29.72 \pm 2.45)\text{Fe (pg)} \quad \text{Equation 10}$$

Re-arranging this yields a minimum amount of iron ≈ 0.2 pg above the physiological amount present within cells.

(vi) Image analysis of Prussian blue images

All image analysis was performed using MacBiophotonics Image J. As the Prussian blue staining images presented in Figure 3 were obtained using a colour CCD camera, the signal in each pixel was saved in red green blue (RGB) format. Image analysis was required in order to compare the Prussian blue signal to that of the photothermal image (saved in 16-bit TIFF format). A colour deconvolution was performed using 'Colour Function' plugin; specifying a blue, pink and white area for each region of interest. Figure S6 presents an example of this processing for cells incubated with 5 $\mu\text{g/mL}$ SPIONs.

After obtaining a greyscale image for the blue channel only, this signal was inverted and a region of interest corresponding to the photothermal image was selected. As the photothermal and Prussian blue images were obtained using different magnifications, it was necessary to scale the pixels in the blue channel so that both images were on the same scale. Figure S8 compares the scaled Prussian blue images for the RGB image, a greyscale image of the signal from the blue channel and the equivalent photothermal image. Once this had been performed it was possible to obtain line profiles of the Prussian blue signal.

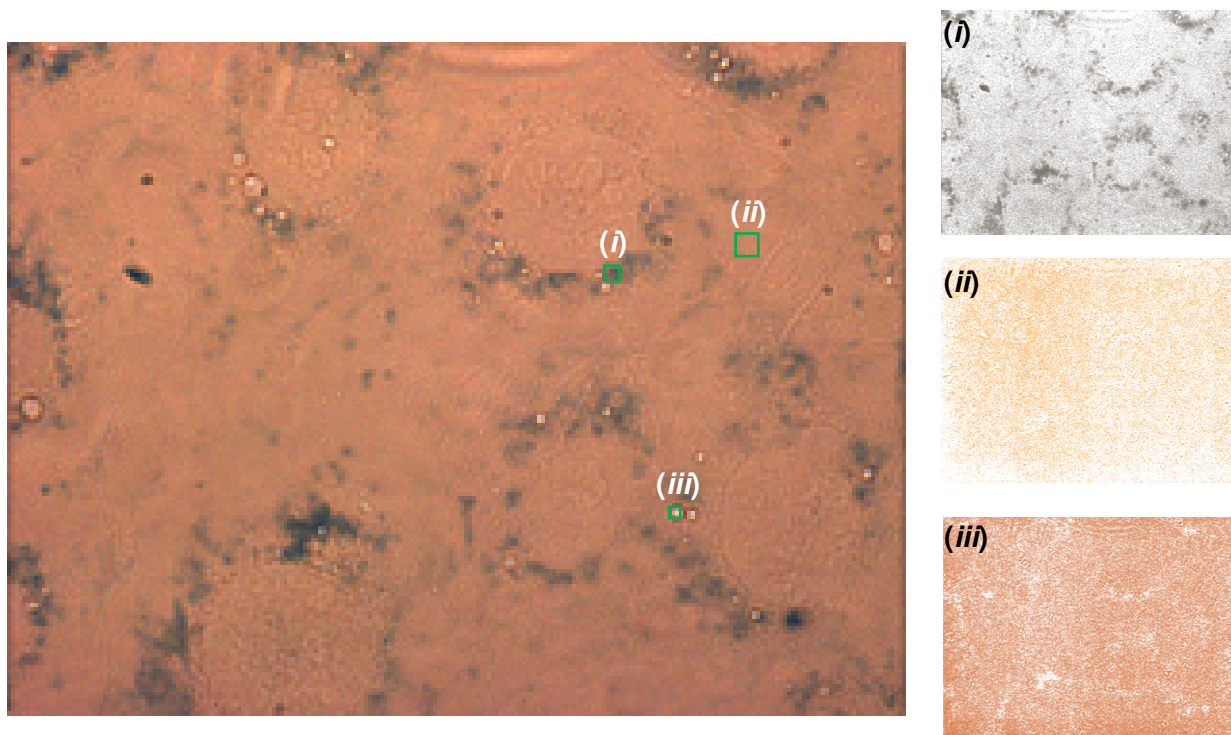


Figure S6. Prussian blue imaging obtained using Thorlabs colour CCD camera for cells incubated with 5 $\mu\text{g/mL}$ SPIONs (*left*). The green squares indicate the three colour regions chosen to deconvolute the image by, and are indicated in the panels (i), (ii) and (iii), respectively. The area shown in (i) corresponds to the blue signal, from which the line profiles presented in Figure 3 were deduced.

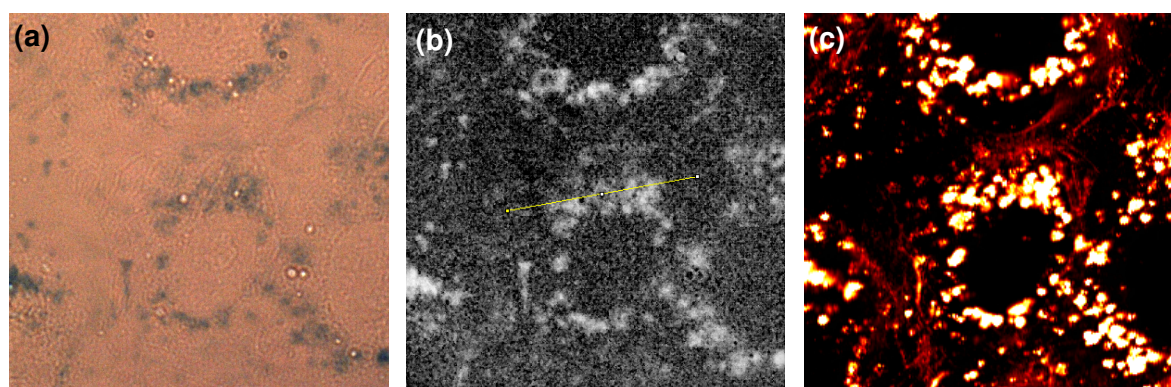


Figure S7. (a) RGB Prussian blue image (b) grey scale image taken from the blue channel using the colour deconvolution technique shown in Figure S6 and (c) photothermal image.

(vii) Cytotoxicity assays

Bright field images were taken immediately before and after photothermal images to look for any changes in morphology typically associated with cell death, an example of which can be seen in Figure S5.

Cell death was assayed using the Sytox[®] nucleic acid stain (Molecular probes). The Sytox[®] comprises a nucleic acid stain which does not cross the membranes of live cells but penetrates cells with a compromised membrane. Dead cells were identified by fluorescence microscopy using a Carl Zeiss excitation filter of 545 nm (bandpass 25 nm) and a Carl Zeiss emission filter of 605 nm (bandpass 70 nm).

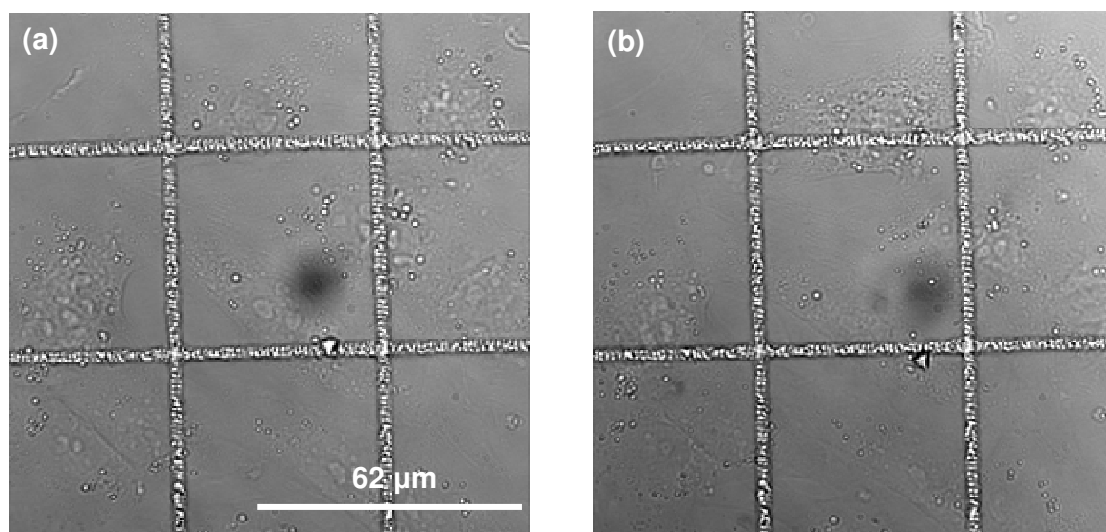


Figure S8. Bright field images (a) before and (b) after photothermal scanning.

Sytox images are presented in Figure S9. The images in panels A-C show that after 5.5 h two dead cells were present in the scanned area. It must be noticed, however, that within a semi-confluent dish there is often a small fraction of the cells population which undergo apoptosis and/or necrosis. The number of dead cells increased with time, but the amount of cell death was the same in the whole dish, which suggests that there is no direct cytotoxic effect of the photothermal imaging. The density of cells increased with time, reaching approximately 90% after 30 h, indicating that the cells in the entire dish (including the scanned areas) were able to proliferate.

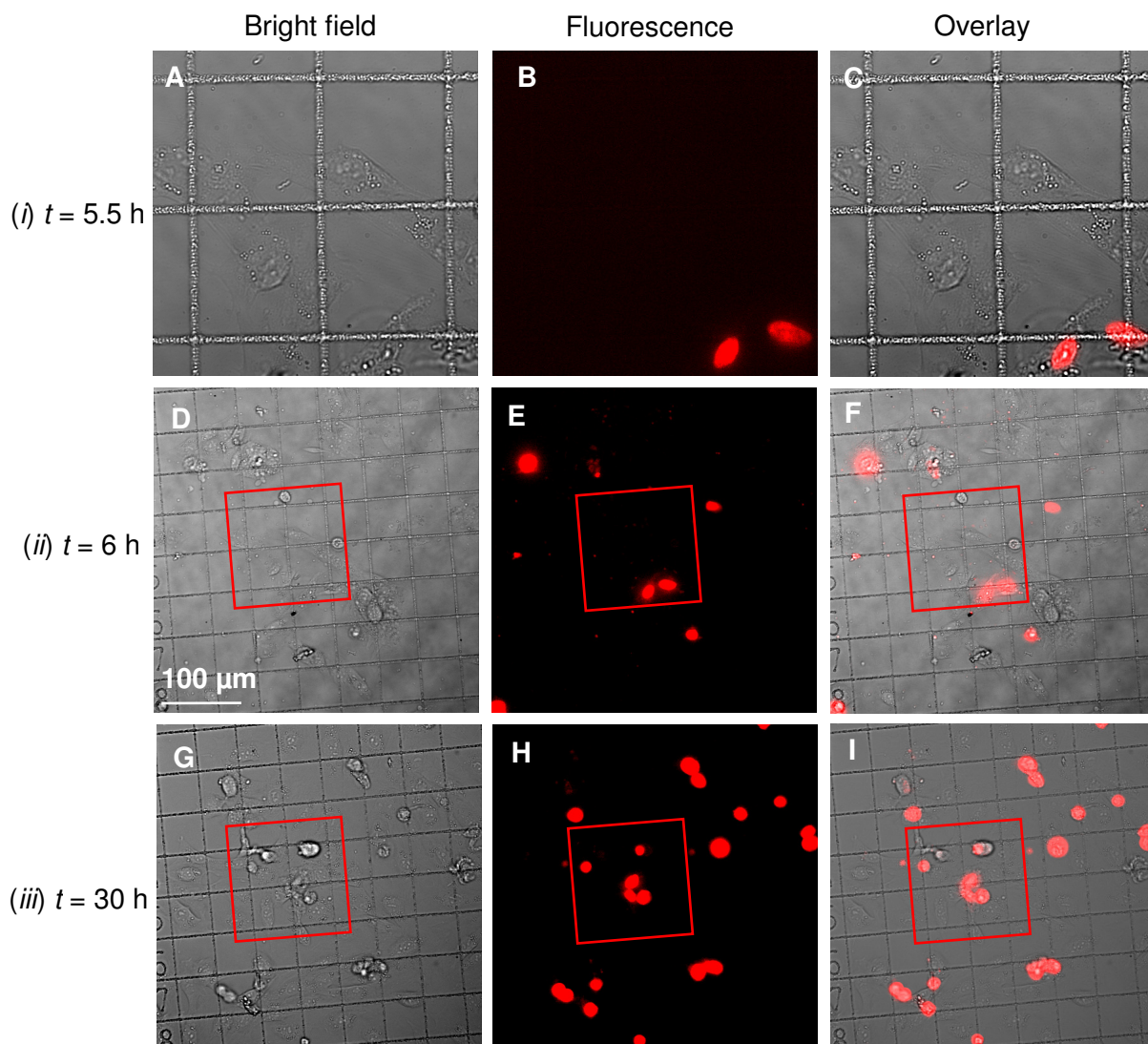


Figure S9. Comparison of bright field imaging, and Sytox® fluorescence imaging for live cells at (i) $t = 5.5$ h, (ii) $t = 6$ h and (iii) $t = 30$ h, where the time corresponds to the delay after the addition of SPIONs. The region indicated by the red square in images (D-I) corresponds to the area scanned during photothermal imaging (shown in A-C); and were taken using a 20x objective to give a larger field of view. After 6 h the area indicated in the square had been scanned 6 times whilst after 30 h it had been scanned 8 times.

(viii) Live cell imaging

Figure S10 presents live cell images of three different fields, all previously imaged 7 times with the photothermal laser.

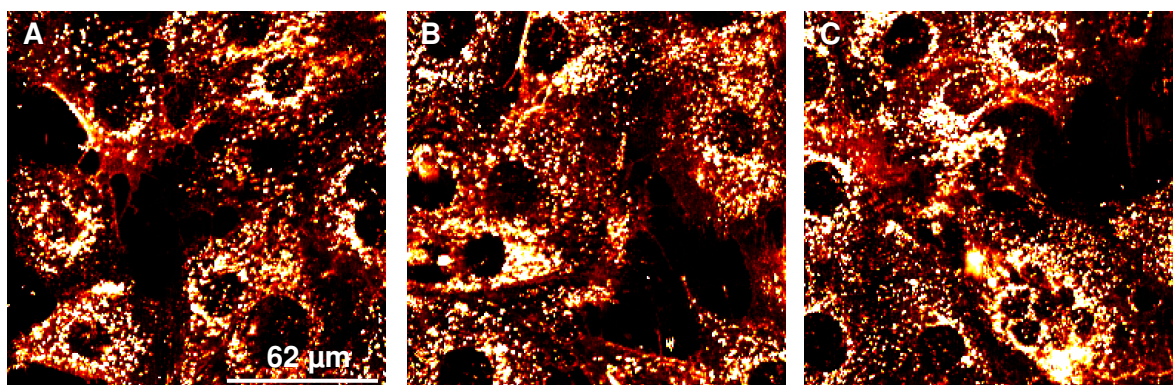


Figure S10. Photothermal images of three different fields taken 1 day after the addition of SPIONs to the cell medium. Each area had been scanned 7 times prior to these images, with all images presented to the same brightness and contrast settings.

(ix) Effect of incubation temperature on endocytosis of SPIONs

Further images taken from cells incubated with 5 $\mu\text{g}/\text{mL}$ SPIONs for 5 h at 4°C and 37°C are provided in Figure S11. In both cases, cells were rinsed and fixed prior to photothermal imaging. There is generally a very low level of signal from the cells incubated at 4°C, suggesting that membrane binding of the particles is reversible and can be easily rinsed away. There is a clear change in the photothermal signal for cells incubated with and without particles.

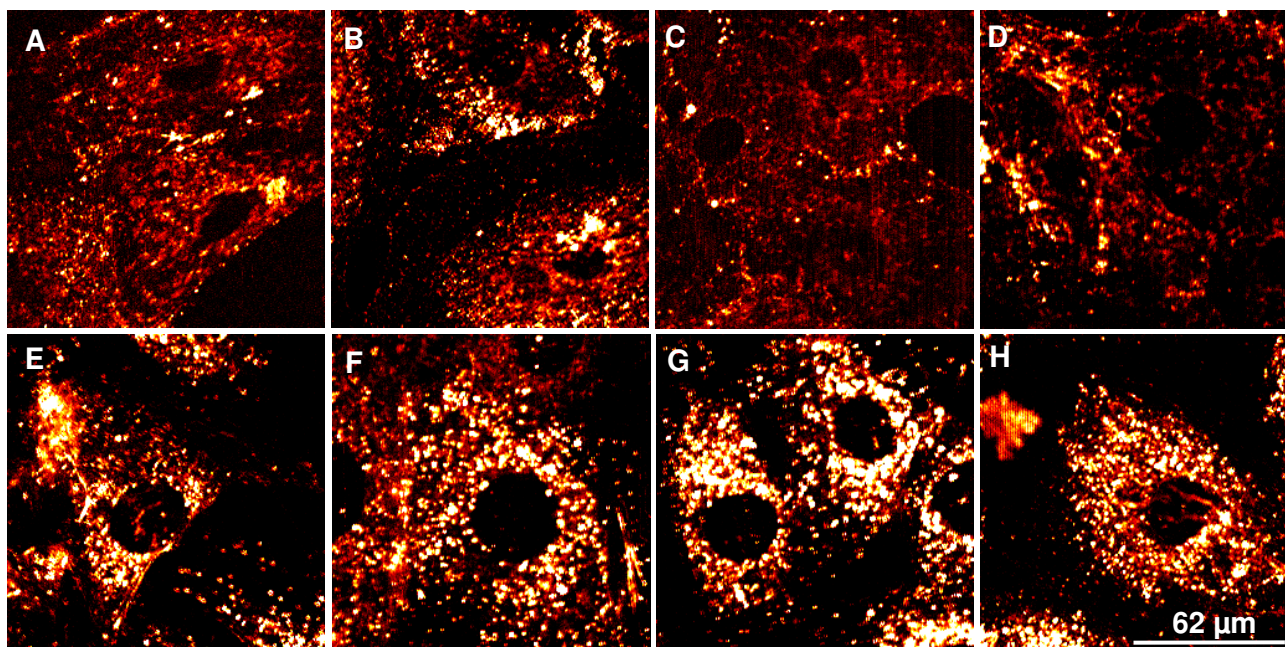


Figure S11. Photothermal images of cells incubated with 5 $\mu\text{g}/\text{mL}$ of SPIONs for 5 h at 4°C (top panel) and 37°C (bottom panel). In both cases, cells were rinsed and fixed prior to photothermal imaging.

ⁱ Smit, J., and Wijn, H. P. J., "*Ferrites*" Wiley (New York) 1959